

IL NUOVO CIMENTO
DOI 10.1393/ncc/i2014-11642-5

VOL. 36 C, N. 6

Novembre-Dicembre 2013

COLLOQUIA: LaThuile13

Search for tb resonances in the leptonic final state with the CMS experiment

D. SPERKA on behalf of the CMS COLLABORATION

Boston University - Boston, MA, USA

ricevuto il 20 Giugno 2013; approvato l'1 Luglio 2013

Summary. — A search for a W' boson is presented using a dataset corresponding to 5.0 fb^{-1} of integrated luminosity collected during 2011 by the CMS experiment at the LHC in pp collisions at $\sqrt{s} = 7 \text{ TeV}$. The W' to tb decay mode is analyzed leading to a final state signature with a single electron or muon, missing transverse energy, and jets, at least one of which is identified as a b-jet. Different scenarios involving an arbitrary mixture of both left-handed and right-handed chiral projections of the fermions are considered. A W' boson that couples to the right-handed (left-handed) chiral projections of the fermions with the same coupling constants as the Standard Model W boson is excluded for masses below 1.85 (1.51) TeV at the 95% confidence level.

PACS 12.60.-i – Models beyond the standard model.

PACS 25.75.Dw – Particle production (relativistic collisions).

PACS 14.70.-e – Gauge bosons.

1. – Introduction

Charged massive gauge bosons, usually referred to as W' , are predicted by various extensions of the Standard Model (SM) [1-5]. For W' bosons that couple only to right-handed fermions, the decay $W' \rightarrow \ell\nu$ will be suppressed if the mass of the right-handed neutrino is larger than the mass of the W' boson. In this case, an important way to search for a W' boson is through the decay to third generation quarks $W' \rightarrow tb$ ($t\bar{b} + \bar{t}b$). Furthermore, in some models the third generation fermions are expected to couple more strongly to the W' than the first and second generations [6].

Previous searches in this channel have been carried out by the D0 experiment at the Tevatron [7] and by the ATLAS experiment at the LHC [8]. If the W' has left-handed couplings, interference between $W' \rightarrow tb$ and SM single-top quark production via $W \rightarrow tb$ can significantly affect the W' production rate [9]. This article describes an analysis using data collected by the CMS experiment corresponding to an integrated luminosity of 5.0 fb^{-1} at $\sqrt{s} = 7 \text{ TeV}$ [10]. The search takes the interference effects into account and puts constraints on an arbitrary set of left- and right-handed couplings of the W' bosons.

2. – Method

2.1. Signal modeling. – The most general model-independent lowest-order effective Lagrangian for the interaction of the W' boson with SM fermions [11] can be written as

$$(1) \quad \mathcal{L} = \frac{V_{f_i f_j}}{2\sqrt{2}} g_w \bar{f}_i \gamma_\mu \left[a_{f_i f_j}^R (1 + \gamma^5) + a_{f_i f_j}^L (1 - \gamma^5) \right] W'^\mu f_j + \text{h.c.},$$

where $a_{f_i f_j}^R, a_{f_i f_j}^L$ are the right- and left-handed couplings of the W' boson to fermions f_i and f_j , $g_w = e/(\sin \theta_W)$ is the SM weak coupling constant, and θ_W is the Weinberg angle. When the fermion is a quark, $V_{f_i f_j}$ is an element of the Cabibbo-Kobayashi-Maskawa matrix, and when it is a lepton, $V_{f_i f_j} = \delta_{ij}$ where δ_{ij} is the Kronecker delta and i and j are the generation numbers. This effective Lagrangian has been incorporated into the SINGLETOP Monte Carlo (MC) generator [9] which simulates electroweak top-quark production processes based on the complete set of tree-level Feynman diagrams calculated by the COMPHEP [12] package, and is used to simulate the s -channel W' signal including interference with the SM W boson.

Arbitrary combinations of left- and right-handed coupling strengths can be accounted for by simulating different samples of s -channel tb production: W'_L bosons that couple only to left-handed fermions ($a_{f_i f_j}^L = 1, a_{f_i f_j}^R = 0$), W'_R bosons that couple only to right-handed fermions ($a_{f_i f_j}^L = 0, a_{f_i f_j}^R = 1$), and W'_{LR} bosons that couple equally to both ($a_{f_i f_j}^L = 1, a_{f_i f_j}^R = 1$). The samples for W'_L and W'_{LR} include the SM s -channel tb production and the interference effects. The W'_R bosons couple to different final-state quantum numbers and therefore there is no interference with s -channel tb production.

The leptonic decays of W'_R require a right-handed neutrino ν_R of unknown mass. If $M_{\nu_R} \ll M_{W'}$, the decay to $\ell\nu$ final states is allowed and leads to a smaller branching fraction for $W' \rightarrow tb$. If $M_{\nu_R} > M_{W'}$, W'_R bosons can only decay to qq' final states.

2.2. Background modeling. – Samples of simulated events are used to estimate contributions from the SM background processes. The W +jets and Drell-Yan ($Z/\gamma^* \rightarrow \ell\ell$) backgrounds are estimated using samples generated with the MADGRAPH generator. The $t\bar{t}$ samples are also generated using MADGRAPH and normalized to the approximate next-to-NLO cross section. Electroweak diboson (WW, WZ) backgrounds are generated with PYTHIA and scaled to the NLO cross section calculated using MCFM. The three single top production channels (tW, s -, and t -channel) are generated with POWHEG and are normalized to the NLO cross section calculation. The s -channel single-top sample is considered as background for the W'_R search, whereas in the search for W' with arbitrary coupling combinations only tW and t -channel contribute to the background. A sample of QCD multijet background events generated using PYTHIA is also included. All parton-level samples are processed with PYTHIA for parton fragmentation and hadronization and the response of the detector was simulated using GEANT.

3. – Data analysis

3.1. Event selection. – The $W' \rightarrow tb$ decay with $t \rightarrow Wb$ and $W \rightarrow \ell\nu$ is characterized by the presence of two b jets with high transverse momentum, missing transverse momenta in the event associated with an escaping neutrino, and a high- p_T lepton.

Jets are clustered using the anti- k_T algorithm with a size parameter $\Delta R = 0.5$ and are required to have $p_T > 30$ GeV and $|\eta| < 2.4$. At least two jets are required in the event, and the leading jet must have $p_T > 100$ GeV and second leading jet is required to have $p_T > 40$ GeV. At least one of the two leading jets is required to be tagged as a b jet.

At least one lepton is required to be within the detector acceptance ($|\eta| < 2.5$ for electrons excluding the barrel/endcap transition region, $1.44 < |\eta| < 1.56$, and $|\eta| < 2.1$ for muons). Muons are required to have relative isolation less than 0.15 and transverse momentum $p_T > 32$ GeV. Electrons are required to have relative isolation less than 0.125 and $p_T > 35$ GeV. The leptons are required to be separated from jets by $\Delta R(jet, \ell) > 0.3$. Events containing a second loose lepton with relative isolation less than 0.2 and a minimum p_T requirement for muons (electrons) of 10 GeV (15 GeV) are rejected.

The QCD multijet background is reduced by requiring $E_T^{miss} > 20$ GeV for the muon + jets channel. A tighter $E_T^{miss} > 35$ GeV requirement is used for the electron channel since the multijet background from events in which a jet is misidentified as a lepton is larger and also due to an E_T^{miss} requirement in the electron channel trigger.

Data-to-MC scale factors (g) are measured using Drell-Yan data and applied in order to account for the differences in the simulation for the lepton trigger, identification and isolation requirements. Scale factors depending on the jet p_T and η related to the b-tagging efficiency and the light-quark misidentification rate are applied on a jet-by-jet basis to all jets in the various MC samples.

Additional scale factors are applied to W+jets events depending on whether a b quark, a charm quark, or a light quark is produced in association with the W boson. These factors are derived using two background dominated data samples: events containing zero b-tagged jets and the inclusive sample after all the selection criteria, excluding any b-tagging requirement. By comparing the W+jets background prediction with the observed data in these two control regions, W+light-flavor jets (g_{Wlf}) and W+heavy-flavor jets (g_{Whf}) scale factors are extracted through an iterative process.

3.2. Event reconstruction. – The sensitivity of the search is enhanced by combining the final state objects to determine the top-quark and W' momentum vectors. The E_T^{miss} is used to obtain the xy -components of the neutrino momentum, and the z -component is calculated by constraining the E_T^{miss} and lepton momentum to the W-boson mass (80.4 GeV). This constraint leads to a quadratic equation in $|p_z''|$. In the case of real solutions, both W candidates are considered. In the case of complex solutions, the E_T^{miss} is minimally modified to give one real solution. In order to reconstruct the top quark momentum vector, the possible W momentum vectors are combined with all of the selected jets in the event. The candidate with mass closest to 172.5 GeV is chosen as the best representation of the top quark. The W' momentum vector is obtained by combining the “best” top-quark candidate with the highest p_T jet remaining after the top-quark reconstruction.

The reconstructed $t\bar{b}$ invariant mass distribution for the observed data, background prediction, and simulated W' signal generated at four different mass values (0.8, 1.2, 1.6, and 1.9 TeV) is shown for the electron and muon channels in fig. 1. Three additional criteria are used to improve the signal-to-background discrimination: the p_T of the best top candidate must be greater than 75 GeV, the p_T of the system comprising of the two leading jets $p_T(jet1, jet2)$ must be greater than 100 GeV, and the best top candidate must have a mass $M(W, bestjet)$ between 130 and 210 GeV.

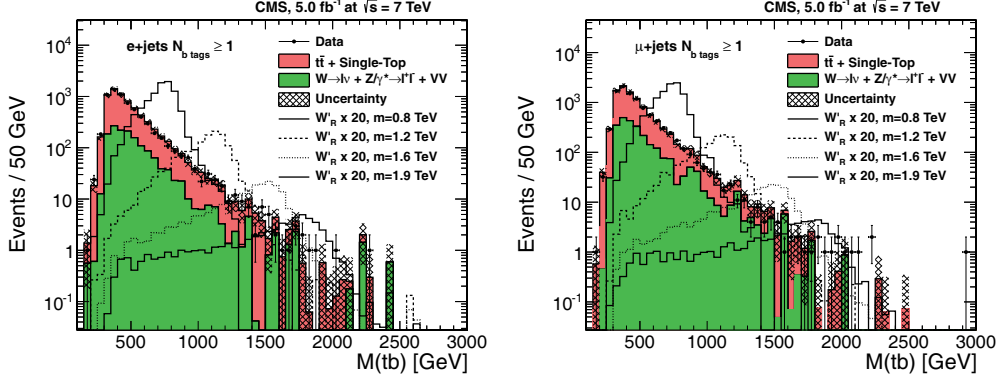


Fig. 1. – Reconstructed W' invariant mass distributions after the full selection. Events with electrons (muons) are shown in the left panel (right panel) for data, background, and four different W'_R signal mass points (0.8, 1.2, 1.6, and 1.9 TeV). The hatched bands represent the total normalization uncertainty in the predicted backgrounds. The expected yields for W' signal samples are scaled by a factor of 20 with respect to the theory prediction.

3.3. Systematic uncertainties. – The sources of systematic uncertainties can affect the shape and normalization of the reconstructed distributions. The uncertainty sources which affect the normalization only are the measured integrated luminosity (2.2%), theoretical cross sections and branching fractions (15%), and the measured efficiencies for the object reconstruction (3%) and trigger selection (3%). The uncertainties which affect both the shape and normalization are the jet energy scale, and the b-tagging efficiency and misidentification rate scale factors. For the W+jets samples, uncertainties on the light- and heavy-flavor scale factors obtained from data are also included, as well as an additional systematic uncertainty due to the shape difference between data and simulation as observed in the 0-b-tagged sample. The variation of the factorization scale Q^2 used in the strong coupling constant $\alpha_s(Q^2)$, and the jet-parton matching scale uncertainties are evaluated for the $t\bar{t}$ background sample.

4. – Results

4.1. Mass limits for generalized coupling strengths. – Based on the effective Lagrangian given in eq. (1), the cross section for single-top quark production in the presence of a W' boson can be expressed in terms of the left-handed (a^L) and right-handed (a^R) coupling strengths, and the cross sections, σ_L , σ_R , σ_{LR} , and σ_{SM} of the four simulated samples as

$$(2) \quad \sigma = \sigma_{SM} + a_{ud}^L a_{tb}^L (\sigma_L - \sigma_R - \sigma_{SM}) + \left((a_{ud}^L a_{tb}^L)^2 + (a_{ud}^R a_{tb}^R)^2 \right) \sigma_R + \frac{1}{2} \left((a_{ud}^L a_{tb}^R)^2 + (a_{ud}^R a_{tb}^L)^2 \right) (\sigma_{LR} - \sigma_L - \sigma_R).$$

The expected W' invariant mass distributions are obtained by combining the four signal samples according to eq. (2) for different combinations of a^L and a^R . For each combination of a^L and a^R we determine the expected and observed 95% CL upper limits

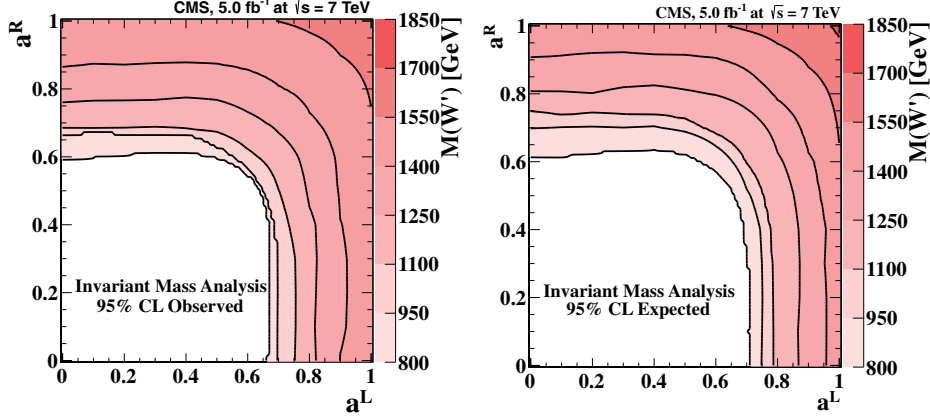


Fig. 2. – Contour plots of $M(W')$ in the (a^L, a^R) plane at which the 95% CL upper cross section limit equals the predicted cross section for the combined e, μ +jets sample. The left (right) panel is for observed (expected) limits. The color-scale axis represents the W' mass in GeV. The dark lines represent 150 GeV intervals of W' mass.

on the cross section as a function of $M(W')$. Figure 2 shows the contours for the W' boson mass in the (a^L, a^R) plane for which the cross section limit equals the predicted cross section. For each contour of W' mass, combinations of the couplings a^R and a^L above and to the right of the curve are excluded. For this analysis, we make the conservative assumption that $M_{\nu_R} \ll M_{W'}$.

4.2. BDT analysis for W'_R . – The boosted decision tree (BDT) multivariate analysis technique is used to distinguish between the W'_R signal and the background. This method provides a considerable increase in sensitivity for the W'_R search compared to the W' invariant mass analysis.

The discriminating variables used for the BDT analysis include object kinematics, event kinematics, angular correlations, and top-quark reconstruction variables. The set of variables used for this analysis is shown in table I. The BDTs are trained separately for the electron and muon event samples after requiring the presence of one or more b-tagged jets at each W' mass. The signal, data and background distributions obtained for a W'_R with mass of 1 TeV, for both e +jets and μ +jets events, is shown in fig. 3.

The modeling in the simulation of the input variables selected for the BDT are checked for accuracy in two different regions dominated by W +jets and $t\bar{t}$ events. The W +jets dominated sample is defined by requiring exactly two jets, at least one b-tagged jet, and the scalar sum of the transverse energies of all kinematic objects in the event to be less than 300 GeV. The $t\bar{t}$ dominated sample is defined by requiring more than four jets, and at least one b-tagged jet.

The BDT discriminant distributions for each mass point are used to set upper limits on the W'_R production cross section. The expected and measured 95% CL upper limits are shown in fig. 4. The sensitivity achieved using the BDT output discriminant is greater than that obtained using the shape of the distribution of the W' boson invariant mass. The observed lower limits on the mass of the W' boson for different W' models is summarized in table II.

TABLE I. – Variables used for the multivariate analysis.

Object kinematics	Event kinematics
$\eta(\text{jet1})$	Aplanarity(alljets)
$p_T(\text{jet1})$	Sphericity(alljets)
$\eta(\text{jet2})$	Centrality(alljets)
$p_T(\text{jet2})$	$M(\text{btag1}, \text{btag2}, W)$
$\eta(\text{jet3})$	$M(\text{jet1}, \text{jet2}, W)$
$p_T(\text{jet3})$	$M(\text{alljets})$
$\eta(\text{jet4})$	$M(\text{alljets}, W)$
$\eta(\text{lepton})$	$M(W)$
$p_T(\text{lightjet})$	$M(\text{alljets}, \text{lepton}, E_T^{\text{miss}})$
$p_T(\text{lepton})$	$M(\text{jet1}, \text{jet2})$
$\eta(\text{notbest1})$	$M_T(W)$
$p_T(\text{notbest1})$	$p_T(\text{jet1}, \text{jet2})$
$p_T(\text{notbest2})$	$p_T(\text{jet1}, \text{jet2}, W)$
E_T^{miss}	$p_z/H_T(\text{alljets})$
Top quark reconstruction	Angular correlations
$M(W, \text{btag1})$ (“btag1” top mass)	$\Delta\phi(\text{lepton}, \text{jet1})$
$M(W, \text{best1})$ (“best” top mass)	$\Delta\phi(\text{lepton}, \text{jet2})$
$M(W, \text{btag2})$ (“btag2” top mass)	$\Delta\phi(\text{jet1}, \text{jet2})$
$p_T(W, \text{btag1})$ (“btag1” top p_T)	$\cos(\text{best}, \text{lepton})_{\text{besttop}}$
$p_T(W, \text{btag2})$ (“btag2” top p_T)	$\cos(\text{light}, \text{lepton})_{\text{besttop}}$
	$\Delta R(\text{jet1}, \text{jet2})$

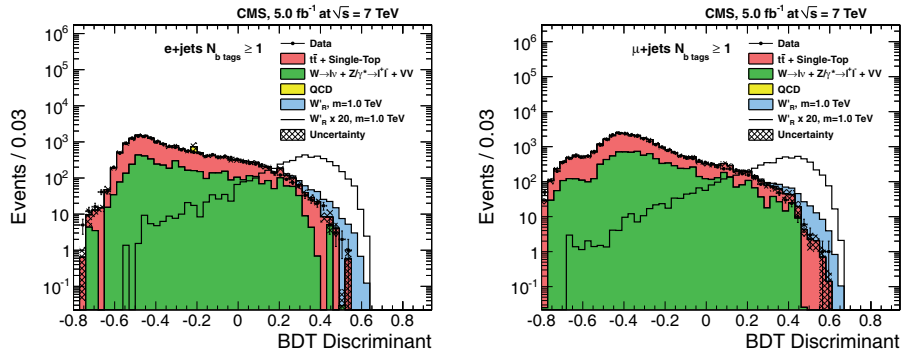


Fig. 3. – Distribution of the BDT output discriminant. Plots for the electron (left) and the muon (right) channels are shown for a W'_R signal with a mass of 1 TeV. The hatched bands represent the total normalization uncertainty on the predicted backgrounds.

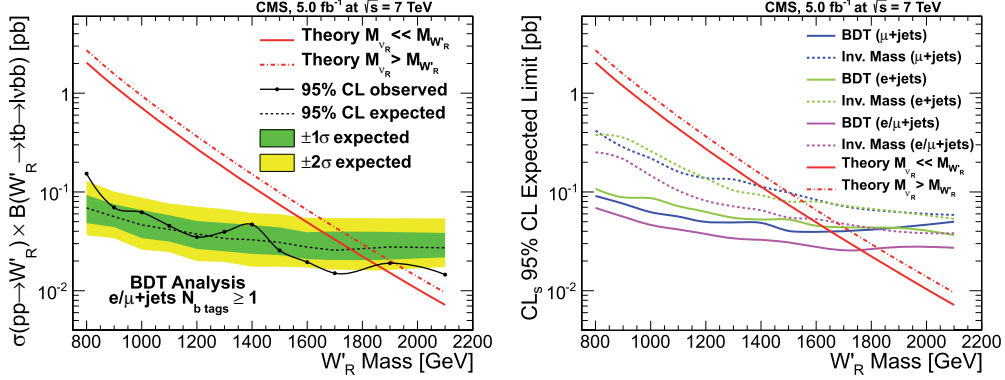


Fig. 4. – The expected and measured 95% CL upper limits on the production cross section $\sigma(pp \rightarrow W')B(W' \rightarrow tb \rightarrow \ell\nu bb)$ of right handed W' bosons obtained using the BDT discriminant. Also shown is a comparison of the expected 95% CL upper cross section limits obtained using the invariant mass distribution and BDT output. The solid and dot-dashed red lines represent the theoretical cross section predictions for the two scenarios $M_{\nu_R} > M_{W'}$ and $M_{\nu_R} \ll M_{W'}$.

TABLE II. – Observed lower limit on the mass of the W' boson. For a W' with right-handed couplings, two cases are considered for the right-handed neutrino: $M_{\nu_R} > M_{W'}$ and $M_{\nu_R} \ll M_{W'}$.

Analysis	$(a^L, a^R) = (0, 1)$		$(a^L, a^R) = (1, 0)$	$(a^L, a^R) = (1, 1)$
	$M_{\nu_R} > M_{W'}$	$M_{\nu_R} \ll M_{W'}$	$M_{\nu_R} \ll M_{W'}$	$M_{\nu_R} \ll M_{W'}$
BDT	1.91 TeV	1.85 TeV	—	—
Invariant Mass	—	—	1.51 TeV	1.64 TeV

5. – Conclusions

A search for W' boson production in the tb decay channel has been performed in pp collisions at $\sqrt{s} = 7$ TeV using data corresponding to an integrated luminosity of 5.0fb^{-1} collected during 2011 by the CMS experiment at the LHC. No evidence for W' boson production is found and 95% CL upper limits are set for arbitrary mixtures of couplings to left- and right-handed fermions. For W' bosons with right-handed couplings to fermions a limit of 1.85 (1.91) TeV is extracted when $M_{\nu_R} \ll M_{W'}$ ($M_{\nu_R} > M_{W'}$). A limit of $M_{W'} > 1.51$ TeV for purely left-handed couplings and $M_{W'} > 1.64$ TeV if both left- and right-handed couplings are present is obtained, assuming $M_{\nu_R} \ll M_{W'}$. During the preparation of this work, updated results on the search for tb resonances were presented by the CMS experiment extending the limit on W' bosons with right-handed couplings to 2.03 TeV [13, 14].

REFERENCES

- [1] SCHMALTZ M. and TUCKER-SMITH D., *Annu. Rev. Nucl. Part. Sci.*, **55** (2005) 229.
- [2] APPELQUIST T., CHENG H. C. and DOBRESCU B. A., *Phys. Rev. D*, **64** (2001) 035002.
- [3] CHENG H. C. *et al.*, *Phys. Rev. D*, **64** (2001) 065007.
- [4] CHIVUKULA R. S., SIMMONS E. H. and TERNING J., *Phys. Rev. D*, **53** (1996) 5258.
- [5] MOHAPATRA R. N. and PATI J. C., *Phys. Rev. D*, **11** (1975) 566.
- [6] MALKAWI E., TAIT T. and YUAN C. P., *Phys. Lett. B*, **385** (1996) 304.
- [7] D0 COLLABORATION, *Phys. Lett. B*, **699** (2011) 145.
- [8] ATLAS COLLABORATION, *Phys. Rev. Lett.*, **109** (2012) 081801.
- [9] BOOS E. *et al.*, *Phys. At. Nucl.*, **69** (2006) 1317.
- [10] CMS COLLABORATION, *Phys. Lett. B*, **718** (2013) 1229.
- [11] SULLIVAN Z., *Phys. Rev. D*, **66** (2002) 075011.
- [12] BOOS E. *et al.*, COMPHEP COLLABORATION, *Nucl. Instrum. Methods A*, **534** (2004) 250.
- [13] HARPER S., *Proceedings of the 48th Rencontres de Moriond QCD* (2013).
- [14] CMS COLLABORATION, *CMS PAS/B2G-12-010* (2013).